

Collagen-Based Fibrillar Multilayer Films Cross-Linked by a Natural Agent

Christophe Chaubaroux,^{†,‡} Engin Vrana,^{†,‡} Christian Debray,^{†,||} Pierre Schaaf,[§] Bernard Senger,^{†,‡} Jean-Claude Voegel,^{†,‡} Youssef Haikel,^{†,‡} Christian Ringwald,^{†,‡} Joseph Hemmerlé,^{*,†,‡} Philippe Lavalle,^{†,‡} and Fouzia Boulmedais[§]

[†]Institut National de la Santé et de la Recherche Médicale, INSERM UMR 977, "Biomaterials and Tissue Engineering", 11 rue Humann, 67085 Strasbourg Cedex, France

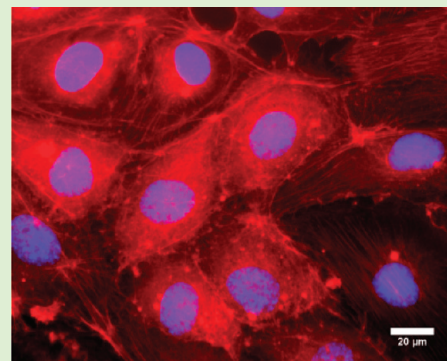
[‡]Faculté de Chirurgie Dentaire, Université de Strasbourg, 1 Place de l'Hôpital, 67000 Strasbourg, France

[§]Centre National de la Recherche Scientifique, CNRS UPR 22, Institut Charles Sadron, 23 rue du Loess, BP 84047, 67034 Strasbourg Cedex 2, France

^{||}Hôpitaux Universitaires de Strasbourg, service d'Oto-Rhino-Laryngologie, 67098 Strasbourg Cedex, France

S Supporting Information

ABSTRACT: Surface functionalization plays an important role in the design of biomedical implants, especially when layer forming cells, such as endothelial or epithelial cells, are needed. In this study, we define a novel nanoscale surface coating composed of collagen/alginate polyelectrolyte multilayers and cross-linked for stability with genipin. This buildup follows an exponential growth regime versus the number of deposition cycles with a distinct nanofibrillar structure that is not damaged by the cross-linking step. Stability and cell compatibility of the cross-linked coatings were studied with human umbilical vein endothelial cells. The surface coating can be covered by a monolayer of vascular endothelial cells within 5 days. Genipin cross-linking renders the surface more suitable for cell attachment and proliferation compared to glutaraldehyde (more conventional cross-linker) cross-linked surfaces, where cell clumps in dispersed areas were observed. In summary, it is possible with the defined system to build fibrillar structures with a nanoscale control of film thickness, which would be useful for in vivo applications such as inner lining of lumens for vascular and tracheal implants.



INTRODUCTION

Polyelectrolyte multilayer (PEM) films constitute surface coatings with well-defined and controlled properties, such as thickness and surface chemistry.¹ In the biomedical field, the approach is often employed to promote cell attachment and to embed bioactive molecules in the film architecture to design gene or drug delivery platforms.² Films can be prepared using synthetic polyelectrolytes, such as poly(styrene sulfonate) (PSS) and poly(allylamine hydrochloride) (PAH). Such films are relatively stiff and thus favor cell adhesion and proliferation.³ But, these polymers cannot be used in the human body because they are not approved by the U.S. FDA and also because of potential inflammatory risks. The development of PEM films using natural polyelectrolytes (polysaccharides or proteins) is of great interest for the design of (bio)materials or surface coatings of devices for medical applications. A number of studies have described the buildup of films with hyaluronic acid (HA), poly(L-lysine) (PLL), chitosan (CHI), or with various proteins such as globular proteins (lysozyme, RNase, IgGs),⁴ bovine⁵ or human serum albumin,⁶ myoglobin,^{7,8} hemoglobin,⁹ and cytochrome C.¹⁰ Cellular adhesion and proliferation on such films, however, are poor,

mainly because of the weak stiffness and high water content of those films.

Collagen (COL) is the most abundant extracellular matrix (ECM) protein present in the mammalian body. It has been used for biomaterial applications in countless forms, mainly as hydrogels,¹¹ foams, and PEM films.¹² In addition to the interaction of its amino acid sequences with cell adhesion receptors, physical properties of collagen have also been shown to play a main role in cellular activities. Collagen, when organized in fibrils, provides structural and mechanical support. Electrospinning is one of the most common nanofibrillar material processing techniques, but there are strong concerns about its effect on collagen denaturation.¹³ COL-based structures are comparable to those found in vivo and may mimic basement membranes where the fibrillar aspect of collagen constitutes an important feature.

Previously, COL-based PEM films were produced with HA,¹⁴ heparin^{15,16} (HN), chondroitin sulfate^{16,17} (CS), PSS,¹⁸ or even

Received: April 4, 2012

Revised: June 4, 2012

Published: June 4, 2012

cellulose nanowhiskers.¹⁹ Alginate (ALG), a natural, degradable polysaccharide as HA, is often employed as a biomaterial.²⁰ To our knowledge, no study was realized on PEM films in which both alginate and collagen were employed. COL/ALG is a system based on natural compounds, both FDA approved, that can be easily dedicated to clinical applications. Thus, combining the properties of collagen and alginate could be of great interest to understand the COL-based multilayer film growth and for future biomedical applications.

Polyelectrolyte films built with polysaccharides and proteins or only polysaccharides raise the problem of their stability in physiological conditions and low stiffness hindering cell adhesion. These drawbacks can be avoided by film cross-linking. Several cross-linking methods exist, such as dehydrothermal treatment, which is not very efficient or chemical cross-linking. Various chemical cross-linkers such as a water-soluble carbodiimide (EDC (1-ethyl-3-(3-dimethylaminopropyl)) in combination with sulfo-NHS (*N*-hydroxysulfo-succinimide),²¹ or bifunctional aldehydes such as glutaraldehyde,²² have been reported. However, cross-linking of natural PEM films carried out with EDC or glutaraldehyde caused significant changes in the physicochemical properties of the films.²³

Genipin, a natural cross-linking agent found in plants, which has been shown to be quite efficient in protein cross-linking,²⁴ represents an alternative of interest. Recently, tissue engineering strategies have used genipin with beneficial side effects, such as control of inflammation²⁵ or enhancement of fibroblastic cells attachment.²⁶

The aim of this work was first to investigate the layer-by-layer film assembly of collagen and alginate, then to characterize the physicochemical properties of the film and finally to stabilize it at physiological pH by genipin cross-linking. We also investigated the adhesion and growth of human umbilical vein endothelial cells (HUVEC) on this innovative multilayer architecture.

■ EXPERIMENTAL SECTION

Materials and Methods. Chemicals and Polyelectrolyte Solutions. Poly(ethyleneimine) was purchased from Sigma Aldrich (PEI, P3143, $M_w = 750\,000$ Da, Saint Quentin Fallavier, France) and was used as a positively charged precursor layer. It was dissolved in 0.15 M NaCl buffer at pH 3.8 (citrate buffer) and deposited for 10 min on the substrate and then rinsed with buffer. Lyophilized collagen (COL, Type I from bovine, medical grade, Symatase, Lyon, France) and sodium alginate (ALG, Pronova UPLVG medical grade, FMC Biopolymers AS Novamatrix, Sandvika, Norway) were dissolved at a concentration of 0.5 g/L in 150 mM NaCl buffer at pH 3.8 (citrate buffer). ALG and COL were deposited alternatively on the substrate with deposition times of 10 and 15 min, respectively, before rinsing. During film construction, all the rinsing steps were performed with an aqueous NaCl solution (150 mM) at pH 3.8 for 5 min. To study the stability of the COL/ALG films at physiological pH, a last rinsing step was performed using a 150 mM NaCl buffer solution (Hepes 10 mM) at pH 7.4. Genipin was purchased from Wako Chemicals (Richmond, U.S.A.) and used without purification. Dimethyl sulfoxide (DMSO) was purchased from Sigma Aldrich. All solutions were prepared using ultrapure water (resistivity of 18.2 M Ω -cm obtained by a Milli-Q water purification system, Millipore).

Chemical Cross-Linking of the Films. Cross-linking was performed on films deposited either on ZnSe crystals (for FTIR-ATR experiments, see below), on SiO₂-coated crystals (for quartz crystal microbalance experiments and atomic force microscopy imaging, see below), or on glass slides (for ζ potential measurements and for cell culture, see below). Glutaraldehyde solutions were prepared in a 150 mM NaCl solution at pH 3.8 (citrate buffer). Genipin solutions were prepared by dissolving the adequate amount of lyophilized genipin

into a DMSO/citrate buffer (150 mM NaCl, pH 3.8) mixture (1:4). The cross-linking agent solution was incubated with the multilayer films for 12 h. Rinsing steps were then performed with citrate buffer at pH 3.8.

Quartz Crystal Microbalance with Dissipation Monitoring (QCM-D). The PEI/(ALG/COL)₃ film buildup and the cross-linking process were followed in situ by quartz crystal microbalance with dissipation monitoring (QCM-D, Q-Sense AB, Göttenborg, Sweden). Briefly, the quartz crystal is excited at its fundamental frequency (about 5 MHz), as well as at the third, fifth, and seventh overtones (denoted by $\nu = 3, \nu = 5, \nu = 7$ corresponding respectively to 15, 25, and 35 MHz). Changes in the resonance frequencies (Δf_i) and in the relaxation of the vibration once the excitation is stopped are measured at these four frequencies. The relaxation gives access to the dissipation D of the vibrational energy stored in the resonator. An increase in $-\Delta f_i/\nu$ is usually associated, in a first approximation, to an increase of the mass coupled to the quartz.

Fourier Transform Infrared Spectroscopy in Attenuated Total Reflection Mode (FTIR-ATR). The cross-linking of PEI/(ALG/COL)₃ films deposited on a ZnSe crystal was investigated by in situ Fourier transform infrared (FTIR) spectroscopy in the attenuated total reflection (ATR) mode with a Vertex 70 spectrophotometer (Bruker, Wissembourg, France). The experiments were performed in a deuterated 150 mM NaCl solution at pH 4. D₂O is used as the solvent instead of H₂O because the amide I band of COL is affected by the strong water absorption band located around 1643 cm⁻¹ (O–H bending), whereas the corresponding vibration in D₂O is found around 1209 cm⁻¹. During the buildup, the film was continuously in contact with the 150 mM NaCl solution. After each rinsing step following a polyelectrolyte deposition and after the final contact with the cross-linking agent solution, single-channel spectra from 128 interferograms were recorded between 700 and 4000 cm⁻¹ with a 2 cm⁻¹ resolution, using Blackman–Harris three-term apodization and the standard Bruker OPUS/IR software (version 3.0.4). Analysis of the raw spectrum was performed at each deposition/rinsing step. During the contact of the film with the cross-linker solution, single-channel spectra from 128 interferograms were recorded at different times.

ζ Potential Measurements. The ζ potential of surfaces was determined with ZetaCAD device (CAD Instrumentation, Les Essarts le Roi, France) and is based on streaming potential measurements. Two glass slides were mounted parallel to each other in a Plexiglas chamber. They were separated by 500- μ m thick poly(tetrafluoroethylene) spacers. The streaming potential was measured 10 times after each layer deposition. The ζ potential was calculated according to the Smoluchowski relation:²⁷

$$\zeta = \frac{\Delta E}{\Delta P} \frac{\eta \lambda}{\epsilon_0 \epsilon_r}$$

where η , λ , ϵ_r , and ϵ_0 correspond respectively to solution viscosity, solution conductivity, relative dielectric permittivity of solution and dielectric permittivity of vacuum. The potential difference ΔE is measured between two Ag/AgCl reference electrodes located on both sides of the measurement cell. The pressure difference ΔP between the electrolyte compartments is varied between -300 and $+300$ kPa with 30 kPa increments. The polyelectrolyte solutions were injected in the measuring cell. Measurements were taken after rinsing with citrate buffer solution (5 mM or 150 mM NaCl, pH 3.8). At the end of the buildup, the cross-linker solution was injected and left in contact for 12 h before rinsing.

Atomic Force Spectroscopy (AFM). Atomic force microscopy (AFM) measurements using a Multimode Nanoscope IV from Bruker (Palaiseau, France) were carried out in contact mode. All images were acquired after a rinsing step with water and drying with a nitrogen flow. Silicon nitride probes (MSCT model, Bruker) with a spring constant of 0.03 N.m⁻¹ were used for imaging. Fibrils thickness was determined by measuring the diameter of 10 individual fibrils in a given image using the ImageJ software and calculating the average thickness and standard deviation (Rasband, W.S., ImageJ, U.S. National Institutes of Health, Bethesda, Maryland, USA, <http://imagej.nih.gov/ij/>, 1997–2011).

Cell Compatibility. Cell Culture. Human umbilical vein endothelial cells (HUVEC, PromoCell, Heidelberg, Germany) were used at passage 4–5 for all experiments. Cell culture was done with endothelial cell growth medium (PromoCell) with supplement mix (heparin, hydrocortisone, basic fibroblast growth factor, epidermal growth factor, endothelial cell growth supplement, fetal calf serum, PromoCell) and 1% penicillin/streptomycin.

The samples were sterilized with UV (30 min exposure) under a tissue culture hood. Near confluent HUVEC cells were removed from flasks with TrypleExpress (Gibco, Villebon-sur-Yvette, France) treatment, counted with a hemocytometer and then seeded onto the films in 50 μL volume with initial cell number of 1×10^4 (proliferation tests) or 5×10^4 (adhesion tests). After an attachment period of 30 min medium was completed to 1 mL and changed daily. Cell attachment, spreading and proliferation were determined by the following tests.

Vybrant Cell Adhesion Assay. For this assay 5×10^4 HUVEC cells labeled with Calcein-AM were used as per instructions of the provider. Briefly, 5×10^6 HUVEC were suspended in 1 mL of growth medium, which then was supplemented with calcein-AM to bring the final concentration to 0.005 mM. Then cells were incubated at 37 $^\circ\text{C}$ for 30 min, washed with medium, and after centrifugation, resuspended. Cellular attachment was checked after 30 min and 1 h of incubation at 37 $^\circ\text{C}$ with a fluorescence microscope Nikon Ellipse TE200 (objective lens 63×1.4 NA). Images were acquired with Nikon Digital Camera (DXM 1200 or DS-Qi1Mc with ATC-1 or NIS-Elements software).

Proliferation Assay. TOX8 (Sigma Aldrich) is a Resazurin-based assay, where cell number can be inferred from the decrease in the absorption of the dye at 600 nm due to metabolic activity. The test was carried out on samples at days 1, 3, and 5 with 2 h of incubation and readings from the supernatant were performed at reference wavelength of 690 nm.

Cell Morphology. After 5 days, cells on films were fixed with 3.7% paraformaldehyde and stained with Hoechst (20 $\mu\text{g}/\text{mL}$, nuclear dye) and TRITC-Phalloidin (1 $\mu\text{g}/\text{mL}$, binds to cytoskeletal actin). For phalloidin staining, cells were previously permeabilized with 1% Triton-X for 3 min and incubated at room temperature for 1 h with phalloidin. Cells were observed with a fluorescence microscope.

RESULTS AND DISCUSSION

Buildup of the Film. The buildup of polyelectrolyte multilayer films based on collagen and alginate was first monitored in situ with QCM-D. Figure 1 depicts the buildup of

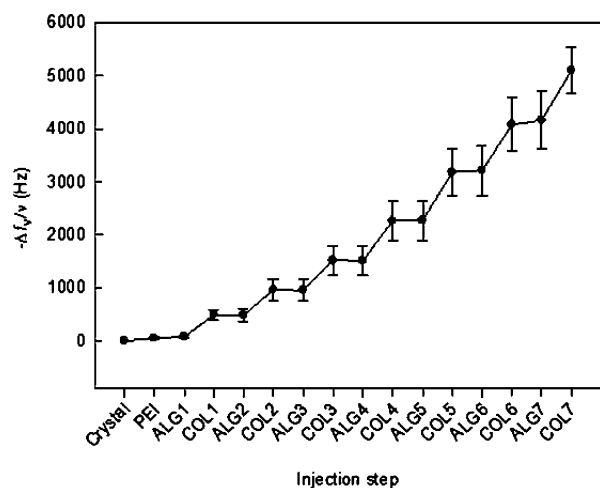


Figure 1. Buildup at pH 3.8 of a PEI/(ALG/COL)₇ multilayer film on a SiO₂-coated crystal followed by QCM-D. Evolution of the opposite of the normalized frequency shift $-\Delta f_i/\nu$ ($\nu = 3$) as a function of the injection step. Error bars correspond to standard deviations determined from three independent experiments.

PEI/(ALG/COL)₇ (7 bilayers) films. Each deposition step of alginate leads to a small increase in the opposite of the normalized frequency noted $-\Delta f_i/\nu$ (Supporting Information S1). This parameter is, in a first approximation, proportional to the mass of polyelectrolytes deposited. Increments in the normalized frequency due to COL injections are greater than the ALG increments. The increment in the normalized frequency because of a COL deposition increases gradually with the number of layers, which indicates that the growth regime of the film is nonlinear. Indeed, it can be verified that the growth regime is exponential up to COL6.

In situ buildup of a PEI/(ALG/COL)₇ film was also followed by FTIR-ATR. Figure 2 shows the spectra acquired after each deposition step. The characteristic bands, amide I, II, and $\delta(\text{CH}_3)/\delta(\text{CH}_2)$, respectively, at 1655, 1560, and 1460 cm^{-1} , were attributed to COL.²⁸ The bands at 1604 and 1415 cm^{-1} were attributed to the antisymmetric and to the symmetric stretching of the COO⁻ groups of ALG.²⁹ The region at 950–1200 cm^{-1} is representative of the skeletal vibrations of saccharide rings of ALG, that is, C–O and C–O–C stretching peaks at 1093 and 1034 cm^{-1} .³⁰ Intensities of all these representative bands increase after each deposition step which demonstrates the layer-by-layer buildup of a PEI/(ALG/COL)₇ film.

Collagen type I, with a pI of 5.5, is positively charged at pH 3.8.³¹ Alginate (pK_a of 3.5) is slightly negatively charged at pH 3.8. Zeta potential measurements of a PEI/(ALG/COL)₃ film during its buildup and after each injection step performed at pH 3.8 in a citrate buffer 150 mM NaCl demonstrate that an overcompensation after each injection step occurs: the ζ potential alternates between negative values (from -4.7 to -1.9 mV) after each ALG injection step and positive values (from $+1.7$ to $+3.3$ mV) after each COL deposition step (Figure 3a). However, the amplitude of this alternation is quite low compared to that of other PEM films.³² This is probably due to the low charge density carried by COL or ALG. Similar measurements, also performed at pH 3.8, but with a lower salt concentration (5 mM) revealed stronger amplitude in signals after each injection step (around 16 mV) (Figure 3b).

Morphology of the Films. Atomic force microscopy images show the formation of a homogeneous film after the deposition of only $n = 3$ pairs of layers (Figure 4a and b). At higher magnification, collagen fibrils are observed (Figure 4b).

Thicknesses of PEI/(ALG/COL)₃ and PEI/(ALG/COL)₇ films reach about 24 and 84 nm, respectively (Supporting Information S2). The layer-by-layer method is ideal to prepare films with a good control of thickness. These results show that it is possible to control the thickness of COL/ALG films at a nanometric scale by changing the number of bilayers deposited.

Stabilization by Chemical Cross-Linking. PEI/(ALG/COL)₃ films have been designed with the final aim to be applied for biomedical purposes. For this reason, after their buildup in acidic conditions (citrate buffer at pH 3.8), the films were incubated in a physiological buffer (HEPES buffer at pH 7.4).

This step was followed by QCM-D (Figure 5) which reveals that a large fraction of the PEI/(ALG/COL)₃ film was dissolved (about 80% in less than 1 min). This is probably due to the collagen chains which become negatively charged at pH 7.4 and thus to the disappearance of the electrostatic attraction with the negatively charged alginate (which remains negatively charged at pH 7.4). The same behavior was observed on the dissipation curves (Supporting Information S3).

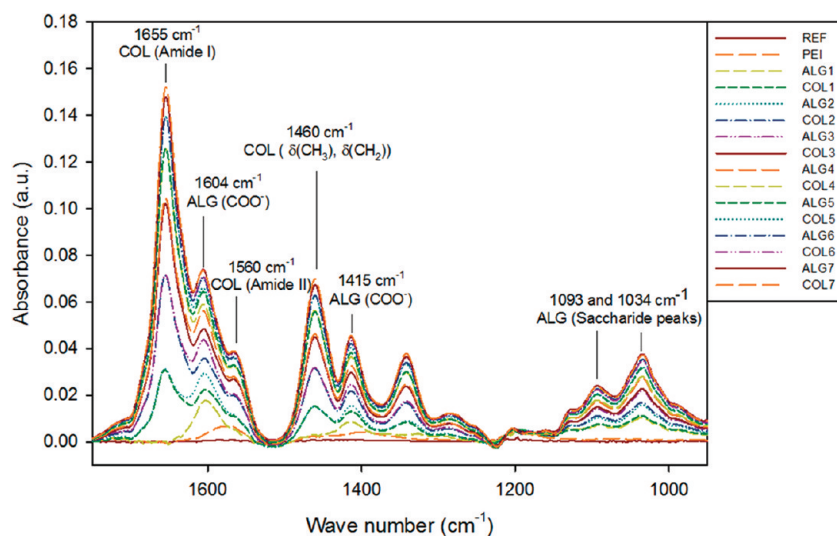


Figure 2. Evolution of FTIR-ATR spectra of a PEI/(ALG/COL)₇ film during its buildup in 150 mM NaCl buffer solution (in D₂O) at pH 3.8. Each spectrum was recorded after each deposition of a layer followed by the rinsing step.

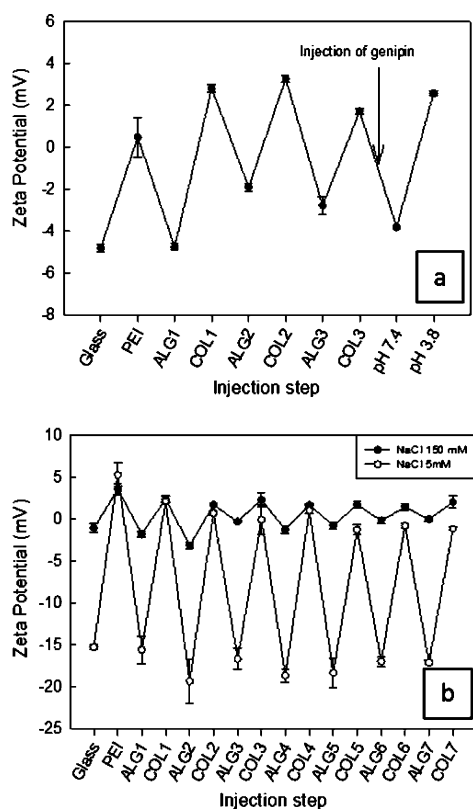


Figure 3. Evolution of the zeta potential of the surface during the buildup of a PEI/(ALG/COL)_n film. (a) PEI/(ALG/COL)₃ film built at an ionic strength of 150 mM NaCl and pH 3.8 (citrate buffer). At the end of the construction, genipin is injected (indicated by an arrow on the graph, $C_{\text{genipin}} = 100$ mM) and then the film was rinsed at pH 7.4 (HEPES buffer) followed by another rinsing step with a citrate buffer at pH 3.8. (b) PEI/(ALG/COL)₇ film built at an ionic strength of 150 mM and 5 mM NaCl. Each mean value corresponds to the average of four measurements and error bars correspond to the standard deviations. The solid lines serve only to guide the eye.

To stabilize these COL/ALG films at physiological pH, genipin, a natural molecule was used. Genipin is becoming of great interest because of its noncytotoxicity and biocompati-

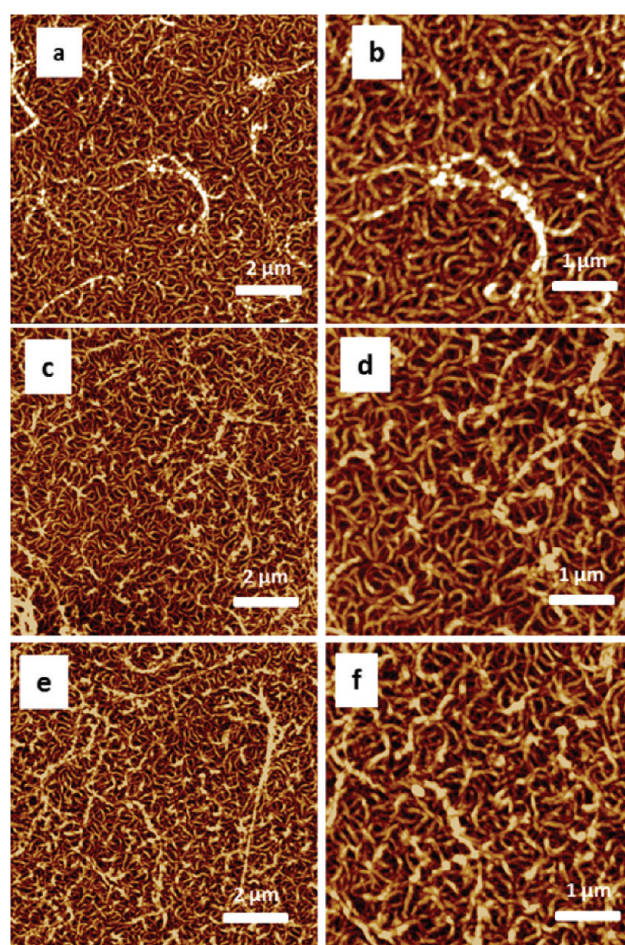


Figure 4. AFM observations of (a) PEI/(ALG/COL)₃ film, (c) PEI/(ALG/COL)₃ film cross-linked with genipin at 100 mM, (e) PEI/(ALG/COL)₃ film cross-linked with glutaraldehyde at 50 mM. Panels b, d, and f are zoomed in views of panels a, c, and e, respectively. Image sizes are $10 \times 10 \mu\text{m}^2$ (a, c, e) and $5 \times 5 \mu\text{m}^2$ (b, d, f), and the z scale is 40 nm.

bility.^{22–24} However, the chemical process of the cross-linking of genipin with an amine-containing compound is not well-

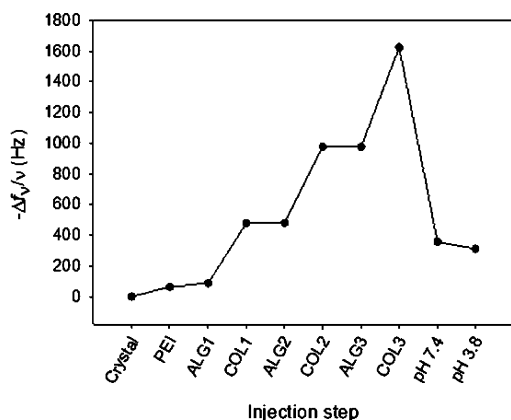


Figure 5. Buildup of a PEI/(ALG/COL)₃ multilayer film on a SiO₂-coated crystal followed by QCM-D. Evolution of the opposite of the normalized frequency shift $-\Delta f_v/\nu$ as a function of the injection step. The buildup is performed at pH 3.8 (citrate buffer) and at the end of the construction, the film is rinsed successively with a HEPES buffer at pH 7.4 and a citrate buffer at pH 3.8.

defined (Supporting Information S4). So far there are still several different mechanisms describing the chemical reaction between the primary amine (chitosan, collagen) and the carboxylic group on genipin.²⁶

The PEI/(ALG/COL)₃ multilayer film was built at pH 3.8 and then incubated overnight in a 100 mM genipin solution (Figure 6). There was only a slight frequency shift after both

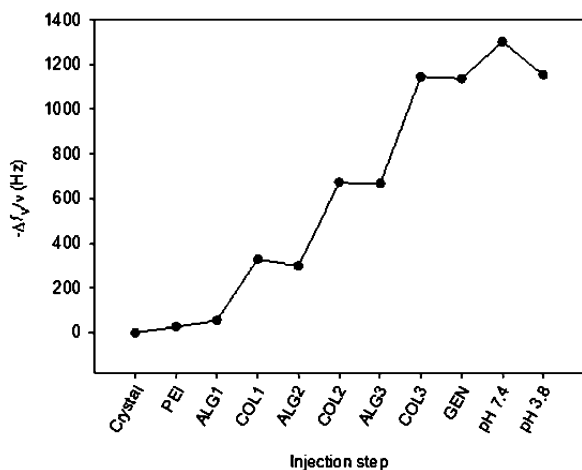


Figure 6. Buildup of a PEI/(ALG/COL)₃ multilayer film on a SiO₂-coated crystal followed by QCM-D. Evolution of the opposite of the normalized frequency shift $-\Delta f_v/\nu$ ($\nu = 3$). The buildup is performed at pH 3.8 (citrate buffer), then genipin (GEN) is put in contact with the architecture at a concentration of 100 mM. Finally, the film is rinsed with a HEPES buffer at pH 7.4, and then brought back to pH 3.8.

genipin injection and rinsing at pH 7.4. However, as soon as the film was brought back to pH 3.8, the frequency measured after film buildup at pH 3.8 was recovered. This clearly indicates that genipin has cross-linked the film preventing dissolution when exposed to a buffer solution at pH 7.4. Thus, the QCM-D measurements confirm the cross-linking suggested by ζ potential measurements (Figure 3a): the results showed that the film resists the pH jump from 3.8 to 7.4, whereas it would have been degraded without cross-linking.

The influence of genipin concentration on the cross-linking ratio was evaluated through QCM-D experiments. PEI/(ALG/COL)₃ films built at pH 3.8 were cross-linked with genipin overnight at concentrations ranging from 5 up to 180 mM, then rinsed with a buffer solution at pH 7.4, and finally rinsed with a buffer solution at pH 3.8. The ratios of the frequencies before and after cross-linking (both at pH 3.8) were evaluated (Figure 7a). Similar experiments were performed with glutaraldehyde (Figure 7b). Glutaraldehyde has been previously used for cross-linking CHI/ALG films to render them more robust.¹

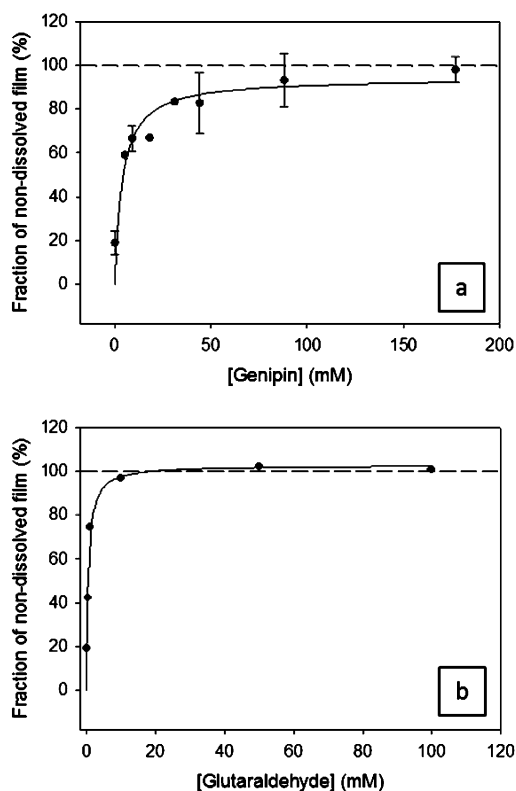


Figure 7. (a) Influence of the genipin concentration on the fraction of nondissolved film for PEI/(ALG/COL)₃ films built at pH 3.8, cross-linked with genipin, rinsed with a pH 7.4 buffer solution and then brought back at pH 3.8. These amounts were evaluated through QCM-D experiments and correspond to “frequency evaluated after cross-linking of the films and rinsing steps at pH 7.4 and pH 3.8”/“frequency evaluated at the end of the buildup of the films at pH 3.8”. (b) Similar to (a) except that cross-linking was performed with glutaraldehyde. Error bars correspond to standard deviations determined from three independent experiments. The solid lines serve only to guide the eye.

For cell culture experiments, the integrity of the films is needed. As indicated in Figure 7a and b, the films are stable once the plateau is reached, independently of the cross-linker concentration. Concentrations of 100 mM (genipin) and 50 mM (glutaraldehyde) were thus chosen to produce films that resist to biological conditions (pH 7.4). PEI/(ALG/COL)₃ films cross-linked with genipin at 100 mM and glutaraldehyde at 50 mM were observed with AFM after rinsing at pH 7.4 and after being brought back to pH 3.8 (Figure 4). Both films reveal similar structures and morphologies than in the native state (without cross-linking), that is, a roughness of about $R_a = 4$ nm and thicknesses of 20–22 nm (Supporting Information S5).

Figure 4c and d show the structure of a COL/ALG film after cross-linking with genipin at 100 mM. The fibrillar structure of the film is preserved and is very similar to the structure of a noncross-linked film, with collagen fibers randomly organized. However, the structure of a COL/ALG film cross-linked with glutaraldehyde at 50 mM is slightly different (Figure 4e and f). The structure is still organized in fibrils, but these are a bit aggregated, which might induce a reduction of available active sites distributed along them. This could be due to glutaraldehyde molecules that make more bonds between the collagen chains than genipin ones during the cross-linking step. The mean diameters of the collagen fibrils are 75 ± 8 nm (uncross-linked), 74 ± 8 nm (cross-linked with genipin) and 82 ± 13 nm (cross-linked with glutaraldehyde). These results indicate that the fibrillar structure of a COL/ALG film is not altered after cross-linking with genipin at 100 mM. Increasing the genipin concentration for cross-linking would probably make the film stiffer due to a large number of bonds between COL chains and thereby render the fibrillar structure like that of a glutaraldehyde-cross-linked film, whereas it is of major importance to keep the collagen fibrils intact for biomedical applications.

COL/ALG film cross-linking was also followed by FTIR-ATR spectroscopy. Genipin (100 mM) or glutaraldehyde (50 mM) solutions were put in contact with PEI/(ALG/COL)₃ films during 12 h. For both cross-linkers, we monitored the spectra of the films in contact with a 150 mM NaCl solution at pH 3.8 before and after cross-linking by genipin (Figure 8a) or by glutaraldehyde (Figure 8b). After cross-linking at pH 3.8, the films were rinsed consecutively with 150 mM NaCl solutions at pH 3.8, pH 7.4, and again at pH 3.8 to remove the noncross-linked material. The difference between the spectra before and after cross-linking is also shown in Figure 8. After cross-linking with genipin (Figure 8a), the absorbance values in the 1410–1500 cm⁻¹ region increase, demonstrating the formation of conjugated alkene and an increase in the CH₃ content (1440 cm⁻¹).³³ A small increase of the band at 1560 cm⁻¹ is visible because of the formation of alkene bonds (stretch of C=C bond) because of the presence of genipin-cross-linked COL (Figure 8a).^{33,34} The decrease of the amide I (1654 cm⁻¹) band of COL and of the carboxylic band of ALG (1604 cm⁻¹) could be explained by a small loss of noncross-linked material during the rinsing step at pH 7.4.

When COL/ALG films are cross-linked with glutaraldehyde (Figure 8b), a small decrease of the carboxylic group band of ALG can be seen at 1604 and 1415 cm⁻¹, probably due to a small loss of noncross-linked ALG after the rinsing at pH 7.4. This result is similar to that found by Alves et al.¹ on CHI/ALG films cross-linked by glutaraldehyde. Imine bonds (C=N) are visible at 1640 and 1670 cm⁻¹ materializing the cross-linking of COL by glutaraldehyde.³⁵

Cell Culture on PEI/(ALG/COL)₃ Films. HUVEC culture was followed on PEI/(ALG/COL)₃ films cross-linked either with genipin at 100 mM or with glutaraldehyde at 50 mM. Initial HUVEC attachment after 1 h of incubation was determined with vybrant cell adhesion assay. Figure 9a and b shows the initial attachment of HUVEC onto glutaraldehyde and genipin-cross-linked samples after 1 h of incubation. Cell attachment is notably better onto genipin-cross-linked samples than on glutaraldehyde ones.

Cell morphology was studied after 5 days of incubation time (Figure 9c and d). Cells are scarcely present onto glutaraldehyde-cross-linked samples. However, onto genipin-

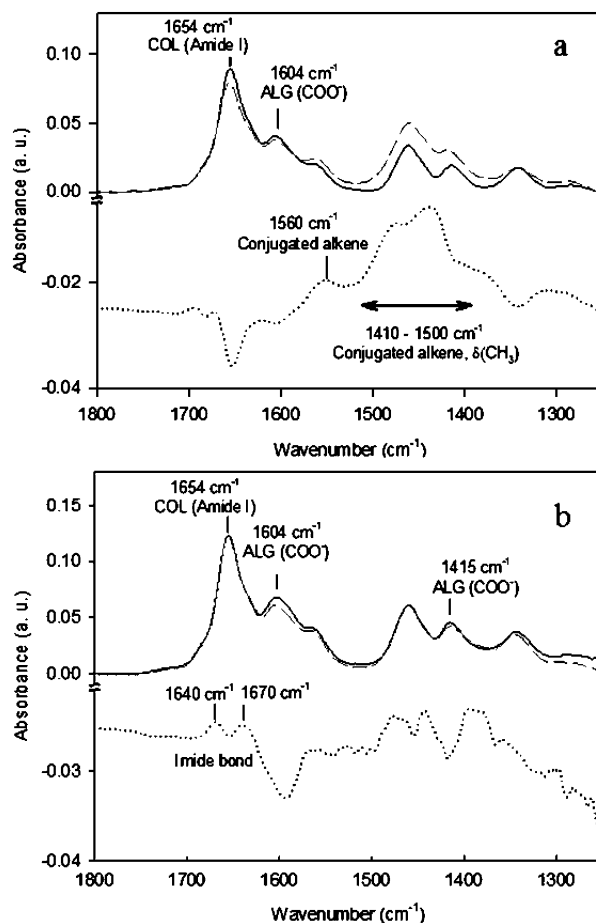


Figure 8. Evolution of the FTIR-ATR spectra of a PEI/(ALG/COL)₃ film before (solid lines) and after cross-linking (dashed lines) with (a) genipin at 100 mM or (b) glutaraldehyde at 50 mM. Dotted lines: difference between the two spectra. The film buildup was performed at 150 mM NaCl in D₂O at pH 3.8. The cross-linking step was followed by a rinsing step at pH 7.4. Then the films were brought back to pH 3.8 before analysis.

cross-linked samples, a confluent HUVEC layer is obtained. Cells seem not only to attach well but also to spread and proliferate well on genipin-cross-linked films. The good proliferation of HUVEC on those films may be due to the good cell attachment in the early period, which is not the case onto glutaraldehyde-cross-linked films.

Proliferation was determined with resazurin-based assay (see Materials and Methods) to determine metabolic activity at 1, 3, and 5 days (Figure 9e). Proliferation results are accompanied by one-way ANOVA tests to show significant differences. Absorption intensities corresponding to glutaraldehyde-cross-linked films are significantly lower than those corresponding to TCPS, independently of the incubation period ($p < 0.05$). On the contrary, absorption intensities corresponding to genipin-cross-linked films are significantly higher than those corresponding to TCPS at day 1 and 3 ($p < 0.01$ at day 3). At day 5, results are quite equivalent as absorption intensities corresponding to genipin-cross-linked films seem to reach a maximum. This may confirm that within an incubation time of 5 days, an endothelial cell layer is formed onto the surface. The cell behavior on genipin-cross-linked films is quite equivalent to the cell behavior on TCPS after 5 days of incubation. Furthermore, absorption intensities corresponding

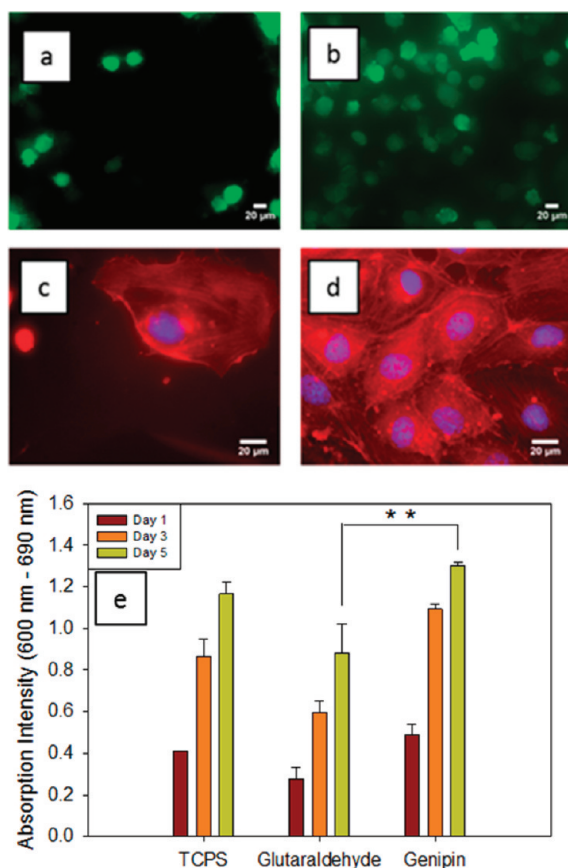


Figure 9. HUVEC behavior on PEI/(ALG/COL)₃ film cross-linked with glutaraldehyde at 50 mM (a and c) or cross-linked with genipin at 100 mM (b and d). (a, b) Initial cell attachment was determined with vybrant cell adhesion assay and calcein-AM staining after 1 h of incubation. (c, d) Cell morphology was studied after 5 days of incubation with Hoechst labeling (nuclear dye = blue) and TRITC-Phalloidin (cytoskeletal actin dye = red). (e) Proliferation was determined with Resazurin-based assay to determine metabolic activity (absorbance of the supernatant at 600 nm-690 nm) at 1, 3, and 5 days. One-Way ANOVA tests were performed for each time of incubation (day 1, 3, 5). The significant difference between absorption intensities of genipin and glutaraldehyde-cross-linked films at day 5 is reported on the graph ($p < 0.01$ indicated by **). For the sake of clarity, significant differences at day 1 and 3 are not reported on the graph but mentioned in the text. Error bars correspond to standard deviations determined from measurements performed in three different wells per condition (i.e., TCPS, genipin-cross-linked films and glutaraldehyde-cross-linked films).

to genipin-cross-linked films are significantly higher than those corresponding to glutaraldehyde-cross-linked ones, independently of the incubation period ($p < 0.001$ at day 3; $p < 0.01$ at day 5, Figure 9e).

These results indicate that genipin-cross-linked PEI/(ALG/COL)₃ surfaces constitute ideal substrates for cellular proliferation. This may originate from the fact that cells sense a surface that contains collagen which mimics ECM. Moreover, genipin, alginate, and collagen are natural and nontoxic molecules, whereas, toxicity of glutaraldehyde toward cells is well-known.³⁶

CONCLUSIONS

We successfully demonstrated the possibility to build collagen/alginate multilayer films, which show a supralinear growth

regime. The cross-linking of such films with genipin, a natural cross-linker, allowed film stabilization at physiological conditions which is of primary importance for their biomedical applications. After cross-linking with genipin, cells adhere better than on films cross-linked with glutaraldehyde. In addition, it was shown that cell proliferation is substantially improved on genipin-cross-linked films compared to TCPS in the early period of incubation. Films based on natural molecules and ECM components could be used in the future as a biocompatible and cell stimulating material to coat prostheses.

ASSOCIATED CONTENT

Supporting Information

Buildup of a PEI/(ALG/COL)₇ film followed by QCM-D. AFM observations of PEI/(ALG/COL)₃ and PEI/(ALG/COL)₇ films, thickness analysis. Buildup of PEI/(ALG/COL)₃ films followed by QCM-D (dissipation curves). Schematic collagen cross-linking reactions by (a) genipin and (b) glutaraldehyde. AFM observation of PEI/(ALG/COL)₃ films cross-linked with either (a) genipin at 100 mM or (b) glutaraldehyde at 50 mM, thickness analysis. This material is available free of charge via the Internet at <http://pubs.acs.org>.

AUTHOR INFORMATION

Corresponding Author

*Phone: +33 (0)3 68 85 33 77. Fax: +33 (0)3 68 85 33 79. E-mail: joseph.hemmerle@inserm.fr.

Notes

The authors declare no competing financial interest.

ACKNOWLEDGMENTS

C.C. is indebted to the Faculté de Chirurgie Dentaire of Strasbourg for financial support. We acknowledge the Région Alsace and the Pôle Matériaux et Nanosciences d'Alsace (PMNA) for financial contribution. We thank K. Benmlih for the buildup of the Zeta Potential cell and C. Bouthier for her assistance.

REFERENCES

- Alves, N. M.; Picart, C.; Mano, J. F. Self Assembling and Crosslinking of Polyelectrolyte Multilayer Films of Chitosan and Alginate Studied by QCM and IR Spectroscopy. *Macromol. Biosci.* **2009**, *9* (8), 776–785.
- (a) Buck, M. E.; Lynn, D. M. Layer-by-Layer Fabrication of Covalently Crosslinked and Reactive Polymer Multilayers Using Azlactone-Functionalized Copolymers: A Platform for the Design of Functional Biointerfaces. *Adv Eng Mater* **2011**, *13* (10), B343–B352. (b) Min, Y. J.; Hammond, P. T. Catechol-Modified Polyions in Layer-by-Layer Assembly to Enhance Stability and Sustain Release of Biomolecules: A Bioinspired Approach. *Chem. Mater.* **2011**, *23* (24), 5349–5357.
- Boura, C.; Muller, S.; Vautier, D.; Dumas, D.; Schaaf, P.; Voegel, J.-C.; Stoltz, J. F.; Menu, P. Endothelial Cell Interactions with Polyelectrolyte Multilayer Films. *Biomaterials* **2005**, *26* (22), 4568–4575.
- Izumrudov, V. A.; Kharlampieva, E.; Sukhishvili, S. A. Multilayers of a Globular Protein and a Weak Polyacid: Role of Polyacid Ionization in Growth and Decomposition in Salt Solutions. *Biomacromolecules* **2005**, *6* (3), 1782–1788.
- Noel, T. R.; Krzeminski, A.; Moffat, J.; Parker, R.; Wellner, N.; Ring, S. G. The Deposition and Stability of Pectin/Protein and Pectin/Poly-L-lysine/Protein Multilayers. *Carbohydr. Polym.* **2007**, *70* (4), 393–405.

- (6) An, Z. H.; Tao, C.; Lu, G.; Möhwald, H.; Zheng, S. P.; Cui, Y.; Li, J. B. Fabrication and Characterization of Human Serum Albumin and L- α -Dimyristoylphosphatidic Acid Microcapsules Based on Template Technique. *Chem. Mater.* **2005**, *17* (10), 2514–2519.
- (7) Pinto, E. M.; Barsan, M. M.; Brett, C. M. A. Mechanism of Formation and Construction of Self-Assembled Myoglobin/Hyaluronic Acid Multilayer Films: An Electrochemical QCM, Impedance, and AFM Study. *J. Phys. Chem. B* **2010**, *114* (46), 15354–15361.
- (8) Miao, X.; Liu, Y.; Gao, W. C.; Hu, N. F. Layer-by-layer assembly of collagen and electroactive myoglobin. *Bioelectrochemistry* **2010**, *79* (2), 187–192.
- (9) Zhang, F.; Liu, L. J.; Wu, Q.; Lin, X. F. Design and in Vitro Biodegradation of Novel Hepatocyte-Targetable (Galactose Polycation/Hemoglobin) Multilayers and Microcapsules. *Macromol. Chem. Phys.* **2009**, *210* (12), 1052–1060.
- (10) Kepplinger, C.; Lisdat, F.; Wollenberger, U. Cytochrome *c*/Polyelectrolyte Multilayers Investigated by E-QCM-D: Effect of Temperature on the Assembly Structure. *Langmuir* **2011**, *27* (13), 8309–8315.
- (11) Kopecek, J. Hydrogel Biomaterials: A Smart Future? *Biomaterials* **2007**, *28* (34), 5185–5192.
- (12) Zhang, J.; Senger, B.; Vautier, D.; Picart, C.; Schaaf, P.; Voegel, J.-C.; Lavalle, P. Natural Polyelectrolyte Films Based on Layer-by-Layer Deposition of Collagen and Hyaluronic Acid. *Biomaterials* **2005**, *26* (16), 3353–3361.
- (13) Zeugolis, D. I.; Khew, S. T.; Yew, E. S. Y.; Ekaputra, A. K.; Tong, Y. W.; Yung, L. Y. L.; Huttmacher, D. W.; Sheppard, C.; Raghunath, M. Electro-spinning of Pure Collagen Nano-Fibres: Just an Expensive Way to Make Gelatin? *Biomaterials* **2008**, *29* (15), 2293–2305.
- (14) Johansson, J. A.; Halthur, T.; Herranen, M.; Söderberg, L.; Elofsson, U.; Hilborn, J. Build-up of Collagen and Hyaluronic Acid Polyelectrolyte Multilayers. *Biomacromolecules* **2005**, *6* (3), 1353–1359.
- (15) Chen, J. L.; Li, Q. L.; Chen, J. Y.; Chen, C.; Huang, N. Improving Blood-Compatibility of Titanium by Coating Collagen–Heparin Multilayers. *Appl. Surf. Sci.* **2009**, *255* (15), 6894–6900.
- (16) Mhanna, R. F.; Vörös, J.; Zenobi-Wong, M. Layer-by-Layer Films Made from Extracellular Matrix Macromolecules on Silicene Substrates. *Biomacromolecules* **2011**, *12* (3), 609–616.
- (17) Gong, Y. H.; Zhu, Y. B.; Liu, Y. X.; Ma, Z. W.; Gao, C. Y.; Shen, J. C. Layer-by-Layer Assembly of Chondroitin Sulfate and Collagen on Aminolyzed Poly(L-Lactic Acid) Porous Scaffolds to Enhance Their Chondrogenesis. *Acta Biomater.* **2007**, *3* (5), 677–685.
- (18) Grant, G. G. S.; Koktysh, D. S.; Yun, B.; Matts, R. L.; Kotov, N. A. Layer-By-Layer Assembly of Collagen Thin Films: Controlled Thickness and Biocompatibility. *Biomed. Microdevices* **2001**, *3* (4), 301–306.
- (19) de Mesquita, J. P.; Patricio, P. S.; Donnici, C. L.; Petri, D. F. S.; de Oliveira, L. C. A.; Pereira, F. V. Hybrid Layer-by-Layer Assembly Based on Animal and Vegetable Structural Materials: Multilayered Films of Collagen and Cellulose Nanowhiskers. *Soft Matter* **2011**, *7* (9), 4405–4413.
- (20) Lee, K. Y.; Mooney, D. J. Alginate: Properties and Biomedical Applications. *Prog. Polym. Sci.* **2012**, *37* (1), 106–126.
- (21) Richert, L.; Boulmedais, F.; Lavalle, P.; Mutterer, J.; Ferreux, E.; Decher, G.; Schaaf, P.; Voegel, J.-C.; Picart, C. Improvement of Stability and Cell Adhesion Properties of Polyelectrolyte Multilayer Films by Chemical Cross-Linking. *Biomacromolecules* **2004**, *5* (2), 284–294.
- (22) Leporatti, S.; Voigt, A.; Mitlohner, R.; Sukhorukov, G.; Donath, E.; Möhwald, H. Scanning Force Microscopy Investigation of Polyelectrolyte Nano- and Microcapsule Wall Texture. *Langmuir* **2000**, *16* (9), 4059–4063.
- (23) Martins, G. V.; Merino, E. G.; Mano, J. F.; Alves, N. M. Crosslink Effect and Albumin Adsorption onto Chitosan/Alginate Multilayered Systems: An in situ QCM-D Study. *Macromol Biosci* **2010**, *10* (12), 1444–1455.
- (24) Bigi, A.; Cojazzi, G.; Panzavolta, S.; Roveri, N.; Rubini, K. Stabilization of Gelatin Films by Crosslinking with Genipin. *Biomaterials* **2002**, *23* (24), 4827–4832.
- (25) Koo, H. J.; Lim, K. H.; Jung, H. J.; Park, E. H. Anti-inflammatory Evaluation of Gardenia Extract, Geniposide and Genipin. *J. Ethnopharmacol.* **2006**, *103* (3), 496–500.
- (26) Hillberg, A. L.; Holmes, C. A.; Tabrizian, M. Effect of Genipin Cross-Linking on the Cellular Adhesion Properties of Layer-by-Layer Assembled Polyelectrolyte Films. *Biomaterials* **2009**, *30* (27), 4463–4470.
- (27) Smoluchowski, M. *Handb. Elektrizität Magn.* **1921**, *2*, 336.
- (28) (a) Vidal, B. D.; Mello, M. L. S. Collagen Type I Amide I Band Infrared Spectroscopy. *Micron* **2011**, *42* (3), 283–289. (b) Belbachir, K.; Noreen, R.; Gouspillou, G.; Petibois, C. Collagen Types Analysis and Differentiation by FTIR Spectroscopy. *Anal. Bioanal. Chem.* **2009**, *395* (3), 829–837.
- (29) Valentin, R.; Bonelli, B.; Garrone, E.; Di Renzo, F.; Quignard, F. Accessibility of the Functional Groups of Chitosan Aerogel Probed by FT-IR-Monitored Deuteration. *Biomacromolecules* **2007**, *8* (11), 3646–3650.
- (30) Gomez-Ordóñez, E.; Ruperez, P. FTIR-ATR Spectroscopy As a Tool for Polysaccharide Identification in Edible Brown and Red Seaweeds. *Food Hydrocolloids* **2011**, *25* (6), 1514–1520.
- (31) Barbani, N.; Lazzeri, L.; Cristallini, C.; Cascone, M. G.; Polacco, G.; Pizzirani, G. Bioartificial Materials Based on Blends of Collagen and Poly(Acrylic Acid). *J. Appl. Polym. Sci.* **1999**, *72* (7), 971–976.
- (32) Picart, C.; Lavalle, P.; Hubert, P.; Cuisinier, F. J. G.; Decher, G.; Schaaf, P.; Voegel, J.-C. Buildup Mechanism for Poly(L-Lysine)/Hyaluronic Acid Films onto a Solid Surface. *Langmuir* **2001**, *17* (23), 7414–7424.
- (33) Mi, F. L.; Shyu, S. S.; Peng, C. K. Characterization of Ring-Opening Polymerization of Genipin and pH-Dependent Cross-Linking Reactions between Chitosan and Genipin. *J. Polym. Sci. Polym. Chem.* **2005**, *43* (10), 1985–2000.
- (34) Madhavan, K.; Belchenko, D.; Tan, W. Roles of Genipin Crosslinking and Biomolecule Conditioning in Collagen-Based Biopolymer: Potential for Vascular Media Regeneration. *J. Biomed. Mater. Res. A* **2011**, *97A* (1), 16–26.
- (35) Yanagawa, H.; Ogawa, Y.; Kojima, K.; Ito, M. Construction of Protocellular Structures under Simulated Primitive Earth Conditions. *Origins Life Evol. B* **1988**, *18* (3), 179–207.
- (36) Ber, S.; Kose, G. T.; Hasirci, V. Bone Tissue Engineering on Patterned Collagen Films: An in Vitro Study. *Biomaterials* **2005**, *26* (14), 1977–1986.